Iraqi Journal of Agricultural Sciences –2026:57(8):2113-2132
P-ISSN: 0075- 0530 /E-ISSN: 2410-0862
DOI: https://doi.org/10.36103/vpe69p76

Synergistic Effect of Rhamnolipid in Nano-Chitosan with Antibiotics Against Multidrug Resistance Skin Pathogens

Osama Akram Dakhil , Nadhim Hassan Hayder
Department of Biotechnology, College of Science, University of Baghdad.

ABSTRACT

This study was aimed to purify and characterize the rhamnolipid biosurfactant produced by an environmental isolate of *P.aeruginosa* (PO10), and to evaluate its antibacterial activity alone in combination with chitosan as nanoparticles. The isolate showed strong hemolytic activity (36.6mm clear zone), high emulsification index (E24%=66). Rhamnolipid was extracted and purified using chloroform: methanol (2:1) solvent system and silica gel column chromatography (3.5 x 30 cm), and was characterized by FTIR and GC-MS. The MIC values of rhamnolipid were 12.5mg/ml for both *P.aeruginosa* and *S.aureus*. Chitosan/rhamnolipid nanoparticles (C/RL-NPs) were synthesized via ionic gelation and characterized by UV-Vis, FTIR, AFM, Zeta potential (+39mV), and FESEM (44.78-60.71 nm, spherical shape).These analyses confirmed the successful formation and high stability of the C/RL-NPs. The MIC of C/RL-NPs was reduced to 1.25mg/ml. This study is the first to investigate the synergistic effect of C/RL-NPs in combination with antibiotics, resulted in significant increases in inhibition zones against both pathogenic isolate of *P.aeruginosa* and *S.*aureus compared to antibiotics or nanoparticles alone.

Key words:antibacterial activity, chitosan, mic,nanoparticles, rhamnolipid, synergistic effect.

Received: 22/3/2025, Accepted: 1/6/2025, Published: 31/8/2026

INTRODUCTION

Multidrug Resistance (MDR) is a serious condition in which microorganisms from various origins exhibit resistance against a wide range of antibiotics. Globally, this situation ranks among the top ten alarming issues (Ohikhena *et al*., 2017). The spread of MDR bacteria is not just nosocomial but also present in the natural environment (Shekhar *et al*., 2015). Nanotechnology refers to the usage and handling of resources that have a size range between 1-100nm known as nanoparticles. In recent years, nanotechnology has been considered as a powerful technology due to its properties which include various magnetic, optoelectronic, and physiochemical characteristics that can be regulated by shape and size distribution (Liu *et al*., 2016). Biosurfactants are amphiphilic molecules that have both hydrophilic and hydrophobic moieties, Surfactants have many applications, including in the food industry, petroleum, cosmetics, sewage treatment, and chemical industry production, as well as the treatment of petroleum-contaminated areas, Surfactants have several advantages, including biodegradability and eco-friendliness, in recent years, biosurfactants have garnered more attention because of their biological properties, versatile functions, emulsifying activity and versatile functions (Prabaharan & Mano, 2005).Biosurfactants have more advantages compared to synthetic ones including their higher biodegradability, thermo stability, lower toxicity, and tolerance to extreme conditions (Vatanparast *et al*., 2018). One of the most popular biosurfactants is glycolipid, that have low molecular weight, and many biotechnological applications consists of two parts, one of them is a carbohydrate and the other is fatty acid chain that linked by glycosidic bond, which serve both hydrophilic and hydrophobic roles. Diversity of glycolipid comes from the differences of carbohydrates and fatty acid chains, subclass of glycolipids are rhamnolipid, sophorolipids, mannosylerythritol lipids, cellobiose lipids, trehalolipids and xylolipids (Niladevi &

Iraqi Journal of Agricultural Sciences –2026:57(8):2113-2132
P-ISSN: 0075- 0530 /E-ISSN: 2410-0862
DOI: https://doi.org/10.36103/vpe69p76

Prema, 2005).Microorganisms which isolated from oil-contaminated soil considered as the majority of glycolipid producers, RL have been confirmed to exhibit potential anticancer effects and are expected to be promising candidates for anticancer drugs (Sifour *et al*., 2007). Another application of rhmanolipids in biomedicine has received more attention in recent years due to their antimicrobial activity against a wide range of bacteria, they considered as safe for recovery of different illnesses, rhamnolipids that derived from *Pseudomonas aeruginosa* isolated from milk factory waste have shown potential use in breast cancer therapy and insect cell line as evaluated by (Varvaresou & Iakovou, 2015) .Chitosan is a polycationic polysaccharide, considered one of the most favorable biopolymers, due to their biocompatibility, biodegradability and lack of toxicity, chitosan has been approved by the FDA for several applications (Costa *et al*., 2021). Chitosan is used to carry antibacterial agents such as antibiotics, anti-inflammatory and anti-cancer agents (Raafat *et al*., 2008). Chitosan nanoparticles have a positive charge and mucous adhesion property, from this property; they can adhere to mucous membranes and release their drugs-loaded (Ali & Ahmed, 2018). Many studies have evaluated chitosan nanoparticles to carry antibiotics and polyphenol products (Hussain *et al*., 2018). An efficient and safe method for producing chitosan nanoparticles is by using Tripolyphosphate (TPP) as a cross-linker, particles are formed by electrostatic interactions between amine groups of chitosan and the phosphate group of TPP. The addition of TPP results in smaller particle sizes also improved loading efficiency, cellular uptake and better bioactivity (Pontes *et al*., 2016). This achievement in glycolipid-chitosan nanoparticles at the laboratory level opens up new avenues to reduce bacteria that resist to antibiotics. This study was designed to synthesize chitosan/rhamnolipid nanoparticles using rhamnolipid biosurfactant produced from *Pseudomonas aeruginosa* which is considered as a reducing and stabilization agent. In addition, to evaluated the biological activity of chitosan/rhamnolipid nanoparticles with some antibiotics in vitro as an antibacterial agent against multidrug resistance pathogens.

MATERIALS AND METHODS

Isolation of *Pseudomonas aeruginosa* from Soil: Twenty two soil samples were collected from University of Baghdad from different locations such as soil contaminated with hydrocarbons (near generators) and oil station, soil was taken from depth of 10cm to avoid surface contamination, suspended in 90ml flask contain sterile normal saline, serial dilutions was prepared by transferring 1ml of the original suspension into 9 ml of sterile saline. 0.1ml of each dilution was transferred into Cetrimide agar using sterile pipette which is considered as a selective media for *pseudomonas aeruginosa*. The isolates were identified by biochemical tests and confirmed by VITEK 2 compact system. Inoculum was spread across the plate with a sterile glass spreader and incubates for 24h at 37°C.

Screening method: Environmental isolates of *pseudomonas sp.* were screened to select higher producing isolates for biosurfactant production, the primary screening was achieved by plate assay using blood agar medium.100 µl of previously activated culture in BHI, were added to each well created in the blood agar medium with 7mm in diameter. The plates were then incubated at 37°C for 24h. The development of a clear zone around wells indicated for biosurfactant production. The radius of the zone was measured in millimeters using an electronic ruler. Secondary screening was tested to obtain the higher rhamnolipid producing isolate, for Emulsification Index (E24%) test. Two ml of cell free supernatant was added into two ml of toluene (equal volumes v/v), mixed with vortex for 2 min, and left for 24 hrs.at room temperature (Abouseoud *et al*., 2008). The emulsifier layer height was determined According to the following equation:

E24%= Height of emulsion layer (mm) / total height of the liquid column (mm) x 100

Production of Rhamnolipid: Batch culture production of RL by selected *P.aeruginosa* isolate was performed in aqueous medium (mineral salt medium), medium components were (CaCO3 (0.02 g/L), CuSO4 (0.009 g/L),

Iraqi Journal of Agricultural Sciences –2026:57(8):2113-2132
P-ISSN: 0075- 0530 /E-ISSN: 2410-0862
DOI: https://doi.org/10.36103/vpe69p76

FeSO4·7H2O (0.01 g/L), K2HPO4 (1.0 g/L), KH2PO4 (0.5 g/L), MgSO4·7H2O (0.6 g/L), NaCl (0.1 g/L), ZnSO4 (5.0 g/L), Olive Oil (2.0% w/v) as carbon source, (2.0% w/v) yeast extract as nitrogen source. The pH was adjusted to 7.0 and then sterilized by autoclaving at 121°C for 15 min. Next, the medium was left to cool and inoculated with 1% ($1x10^8$ CFU/ml) of pre activated *P.aeruginosa* inoculum. Then, it was placed in shaker incubator set at 30°C with 120 rpm for 72 hours in purpose of production of extracellular rhamnolipid (Shaban, 2016).

Optimization of Carbon Source: Different carbon sources were used in fermentation media (MSM) to choose the best carbon source for the production of extracellular rhamnolipid from *P.aeruginosa.* Each of these sources was added to the medium in (2g/100ml) or (2ml/100ml) v/v) including olive oil, black seed oil, glucose and glucose + glycerol (1:1 w/w). Then the medium pH was adjusted to 7.0, shaker incubator was adjusted to 120 rpm, at 30°C for 72hours. After that, the media was inoculated with 1% of overnight culture $1x10^8$ cell/ml (O.D 600 nm) of the selected isolate, E24% was measured to choose the best carbon source for the production of biosurfactant from selected isolate (Pan *et al*., 2020).

Optimization of Nitrogen Source: Nitrogen is important parameter that effect on growth and production of biosurfactant. Nitrogen sources were investigated by adding 2% of different nitrogen sources to the fermentation medium (MSM) such as yeast extract, KNO3, NANO3 and NH4CL + Peptone. A 1% of pervious activated *P. aeruginosa* (OD = 0.5, $1x10^8$ CFU/ml) was suspended in 50 ml of sterile production medium (MSM) containing 2% of the best carbon source and examined nitrogen source at pH 7 and placed in a shaker incubator at 30°C, 120rpm for 72 hours. The emulsification index (E24%) was measured.

Rhamnolipid extraction: The rhamnolipid production was conducted in optimum conditions, such as pH=7, agitation rate 120rpm, at 30°C for 72h, the optimum conditions of rhamnolipid production were described by (Karamchandani *et al*., 2022). After centrifugation with 10000 rpm for 10 min, the collected supernatant containing biosurfactant was transferred to separating funnel and extracted with solvent system chloroform and methanol with ratio (2:1 v/v). The solvents layer at the bottom of the separating funnel was removed, and the emulsion layer was collected in glass petri dish. Then, the collected layer was dried in oven at 50°C. After drying process, the resulting product was collected from petri dishes using sharp tool. The product was weighed and stored in a clean vial at 5°C in refrigerator for further use (Singh *et al*., 2013).

Purification of Rhamnolipid: The extracted RL was purified using silica gel column, where the silica was activated by heating in an oven at 80°C for 4 hrs. Then suspended in organic solvents (chloroform: methanol) at a ratio of (1:1 v/v), the gel was filed in the column with dimensions of (3.5 x30 cm). One gram of rhamnolipid was poured on the slurry after dissolving it in 10 ml of chloroform and methanol 1:1 (v/v), and the mixture of chloroform /methanol was continuously added until all neutral lipids were eluted. One volume of chloroform/methanol (150 mL) was sequentially added to the column at ratios of 50:50 to elute all rhamnolipid at a flow rate of 3 mL/9min. Solvent evaporation was done to remove residual solvents, followed by measuring E24% of the eluted fractions. The separated biosurfactants were then characterized using FTIR and GC-Mass technique to confirm the complete separation and presence of the rhamnolipid (Santa Anna *et al*., 2002).

Characterization of Rhamnolipid (FTIR, GC-MS): The FTIR spectra of the biosurfactant were analyzed within the wavelength range of (500-4000) wave number /cm. The analysis was conducted using a Shimadzu-I Rafffinity-1 spectrophotometer. Additionally, FTIR spectroscopy provides detailed information about molecular bonds and functional groups that have a permanent dipole moment (Pasieczna-Patkowska *et al*., 2025). Also, biosurfactant was analyzed for their fatty acid composition using gas chromatography (GC). Fatty acid methyl esters (FAMEs) were extracted with hexane and analyzed by GC, employing helium as the

Iraqi Journal of Agricultural Sciences –2026:57(8):2113-2132
P-ISSN: 0075- 0530 /E-ISSN: 2410-0862
DOI: https://doi.org/10.36103/vpe69p76

carrier gas. The analysis was performed on a Shimadzu 17-A system equipped with a fused silica capillary column.

Determination of Minimal inhibitory effect of Rhamnolipid (MIC): MIC was determined as the lowest concentration of RL at which the tested microorganism does not demonstrate visible growth. After preparation and activation of selected pathogenic isolate (*S. aureus* and *P. aeruginosa*) isolated from burns and wounds infection, the minimal inhibitory effect of biosurfactant was determined using microtiter plate method. Different concentration of glycolipid was prepared (100, 50, 25, 12.5, 6.2, 3.1, 1.5 and 0.75 mg/ml) using Muller Hinton Broth (MHB) as a diluent. The microtiter plate wells were set up as follows:

Wells from 1 to 8 contained 10µl of bacterial suspension for each pathogenic isolate corresponding to the McFarland standard no. 0.5 (1.5 x 10^8 CFU/ml) with 100µl of each selected concentration of rhamnolipid. The microtiter plate was then incubated for 24 h at 37°C. The positive control well contained Muller Hinton Broth (MHB) 190 µl and 10µl of bacterial suspension without rhamnolipid, while the negative control well contained 200µl of MHB only. In order to detect color change, a 30µl of Resazurin dye was added to each well and incubated for two hours. The MIC of rhamnolipid was determined based on the color shift from blue to pink (Paulino *et al*., 2016).

Antibacterial activity of Rhamnolipid: Well diffusion method was used to determine the best concentration of rhamnolipid against both Gram positive and negative bacteria (*P.aeruginosa* and *S.aureus*). First of all, the selected clinical bacteria isolates were prepared by inoculating tubes containing 10ml of nutrient broth separately with 1:100 of an overnight cultural isolate containing about 1×10^8 cells/ ml. Muller Hinton agar medium was prepared and allowed to solidify (Balouiri *et al.,* 2016). After that, 20µl of selected isolate was spread on Muller Hinton Agar using sterile swab and allowed to dry for 7 min. Four agar wells with diameter 5mm were prepared for each agar plate using sterile cork borer. The wells were labeled for each prepared concentration of RL (100mg/ml, 75mg/ml, 50mg/ml and 25mg/ml). Each well was loaded with 100µl of different rhamnolipid serial dilution and incubated for 24h at 37°C. After incubation period, the inhibition zone was observed and calculated using electronic ruler.

Synthesis of chitosan nanoparticles encapsulated rhamnolipid (C/RL-NPs): Ionic gelation method was used, sodium tripolyphosphate considered as a crosslinking agent. The preparation of chitosan solution 2mg/ml was prepared by dissolving 0.2 g of commercial chitosan in a 100 ml of deionized water and adding 1ml of 1% acetic acid under magnetic stirring for 2-3 hours until the solution became fully clear, ensuring that all chitosan had dissolved. Millipore filter 0.45µm was used to achieve cell-free solution. The solution was then stored in a dark environment to prevent oxidation. The rhamnolipid solution with concentration 3mg/ml was prepared by dissolving 75mg of purified rhamnolipid in 25ml deionized water at pH 5.5. The RL solution was then filtered using 0.45 µm membrane filters (Bettencourt *et al*., 2021). The C/RL NPs was prepared by mixing the chitosan and rhamnolipid solutions at a 1:1 (v/v) ratio under magnetic stirring at 700rpm and 25 °C for 24h. Subsequently, a 3ml of TPP solution 0.5mg/ml with pH 9.5(to assure that all phosphate ions are in the ionized state) were added into C/RL mixture after sterilization using 0.22 µm membrane filters under the same condition of stirring and temperature. The final pH of solution was optimized to 5.5. The NPs were then separated by centrifugation at 14,000 rpm for 20 min and washed triple with deionized water to remove any unbound materials of reaction and remove acetic acid. The nanoparticles obtained after the washing and centrifugation process was then poured into sterile glass dishes and incubated in oven at 40°C for 2 h for drying. The NPs was then removed from dishes using sterile sharp tool and stored in universal tube in dark place for further experiments (Mnif *et al*., 2018).

Characterization of (C/RL-NPs): The physicochemical properties of nanoparticles are important for their behavior, bio-

Iraqi Journal of Agricultural Sciences –2026:57(8):2113-2132
P-ISSN: 0075- 0530 /E-ISSN: 2410-0862
DOI: https://doi.org/10.36103/vpe69p76

distribution, safety, and efficacy. Therefore, characterization of C/RL-NPs is important in order to evaluate the functional aspects of the synthesized particles. UV-visible spectroscopy was used to confirm the formation of C/RL-NPs. Furthermore, Fourier transform infrared spectroscopy (FT-IR) measurements were recorded to identify the major functional groups, Zeta potential to evaluate the stability and surface charge of the C/RL-NPs (Corbett *et al*., 2012) , Atomic force microscopy (AFM) for the determination of nanoparticles surface morphology and mean size (Grobelny *et al*., 2011) and FESEM to analyze the morphology of formed NPs (Ahmad *et al*., 2021).

Determination of Minimal Inhibitory Effect of C/RL-NPs (MIC) Microtiter Plate Method: The MIC was defined as the lowest concentration of C/RL-NPs that completely inhibited the visible growth of tested microorganism. After preparing and activating the selected isolates (*P.aeruginosa*, *S.aureus*), the minimal inhibitory effect of the C/RL-NPs was assessed using the microtiter plate method. 2.5mg/ml stock solution of C/RL-NPs was prepared using 50% DMSO as a solvent and pH of final solution was measured. The microtiter plate wells were set up as follows: The positive control well contained 190 µl of MHB and 10µl of bacterial suspension without C/RL-NPs, while the negative control well contained 200µl of MHB. Other wells from 1 to 10 contained 10µl of bacterial suspension for each pathogenic isolate corresponding to the McFarland standard no. 0.5 (1.5 x 10^8 CFU/ml) and 100 µl of MHB. One hundred µl of C/RL-NPs stock solution (2.5mg/ml) was transferred to the first well and mixed using micropipette. Half of the volume from first well was transferred to the second well, then the process was repeated from the second well to the third, continuing the pattern until reaching well number 10 in microtiter plate. The microtiter plate was then incubated for 24 h at 37°C. In order to detect color change, a 30µl of Resazurin dye was added to each well and incubated for two hours, The MIC of C/RL-NPs was determined based on the color shift from blue to pink**.**

Well Diffusion Method: For more accurate and confirmed results, the antibacterial activity of the produced C/RL-NPs was assessed on agar plates. Firstly, each of selected bacterial isolates (*P.aeruginosa* and *S.aureus*) was corresponding to the McFarland standard no. 0.5 (1.5 x 108 CFU/ml). Then, 20µl of the selected isolate was spread on MHA using sterile swab and allowed to dry for 7 min. Five agar wells with diameter 5mm were prepared for each agar plate using sterile cork borer. The wells were labeled for each concentration (2500µg/ml, 1250µg/ml, 625µg/ml, 312µg/ml, and 156µg/ml) of C/RL-NPs. Each well was loaded with 100µl of different C/RL-NPs concentrations and incubated for 24h at 37°C. After incubation period, the inhibition zone was observed and calculated using electronic ruler.

The Synergistic Effect of C/RL-NPs and Standard Antibiotics: The antibacterial activity of C/RL-NPs in combination with standard antibiotics was evaluated by impregnating of antibiotic disks with 100µl of C/RL-NPs stock solution (concentration depended on result of MIC). The overnight cultures of *S. aureus* and *P. aeruginosa* were adjusted to a final concentration of (1x108 CFU/ml) and spread on the surface of Muller Hinton Agar plates (MHA). A different antibiotic disk was used for each MHA plate, with selected isolates. The disks were left for 10min to allow absorption. Additionally, a 5mm well was created using sterile cork borer and filled with 100 µl of C/RL-NPs only at the same concentration on the same plate. The plates were incubated at 37°C for 24 hrs. All antibiotics disks were supplied by Himedia (India) and selected based on CLSI 2024 guidelines. All experiments were carried out in duplicate, and the inhibition zone was measured using electronic ruler.

RESULTS AND DISCUSSION

Identification of the biosurfactant Producing isolate: Twenty-two soil samples were collected from different sources. The samples were initially cultured on MacConkey agar plates as differential medium and Cetrimide agar as selective medium, and then incubated at 37 °C for 24 hr. Only 13 samples tested gave positive results for *P.aeruginosa*. All isolates were identified using biochemical

Iraqi Journal of Agricultural Sciences –2026:57(8):2113-2132
P-ISSN: 0075- 0530 /E-ISSN: 2410-0862
DOI: https://doi.org/10.36103/vpe69p76

test, and confirmed by VITEK 2 system with 95% similarity.

Screening of *Pseudomonas aeruginosa* isolates for rhamnolipid production: Primary screening (Hemolysis test): All obtained environmental isolates were produced β-hemolysis but in different rate of lysis zones on blood agar except PO 4 and PO18. PO10 showed the highest hemolysis zone with 36.6mm in diameter. Rapid, visible and convenient method for rhamnolipids detection is very important and essential for the high-throughput screening of rhamnolipids-producing *P.aeruginosa* isolates. PO10 has a longer attached hydrophilic chain as compared with other tested strains, since the surfactants that have this property typically have greater hemolytic activity (Bustelo *et al*., 2017).

Secondary screening

Emulsification index (E24%) Test: Eight of isolates (PO6, PO9, PO10, PO12, PO13, PO14, PO15, and PO17) that showed highly hemolysis zone in primary screening were subjected to secondary screening (E24%) test. Emulsification index was calculated to choose the highest rhamnolipid producing isolate. The result in table1, indicate that PO10 isolate showed the highest E24% value which was 66%. Isolate that have higher emulsification index refer to higher producing ability of biosurfactant (Manna *et al*., 2021).

Table 1. Secondary screening of rhamnolipid produced by *P.aeruginosa* using Emulsification index (E24%).

No. of isolate	E24%
PO 6	65
PO9	62
PO 10	66
PO 12	62
PO 13	65
PO 14	58.3
PO 15	63
PO 17	64

Antibacterial activity test

Four isolate (PO 6, PO10, PO15, PO13) that showed highest E24% activity, were tested for their antibacterial activity against pathogenic isolates *P.aeruginosa* and *S.aureus*. Against *S.aureus*, biosurfactant produced from PO10 isolate showed higher antibacterial activity with an inhibition zone of 12.8mm followed by PO15 with 12.3mm, while against *P.aeruginosa* only PO10 showed an inhibition zone of 10mm (figure 1). Therefore, the isolate P.O10 was selected for the remaining experiments in the current study.

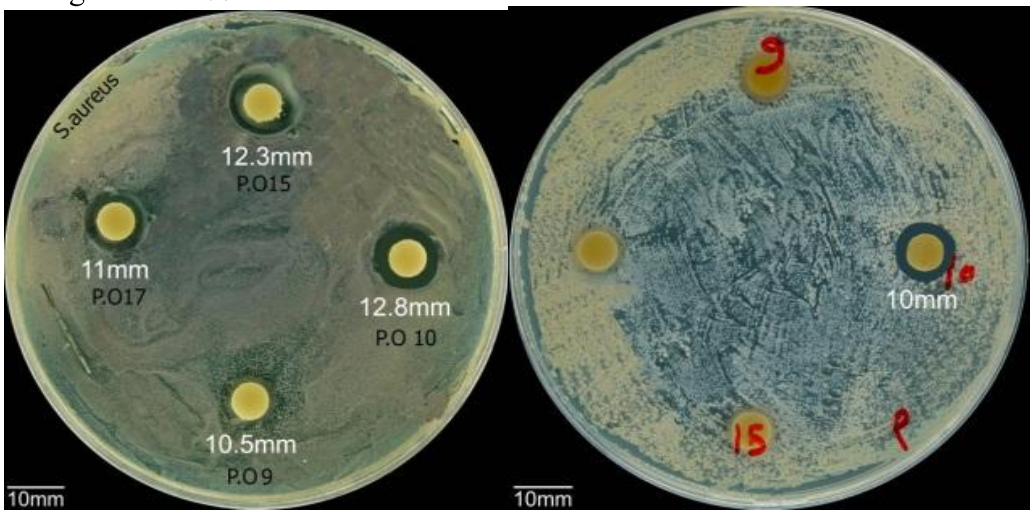

Figure 1. Antibacterial activity of biosurfactant against (A) *Staphylococcus aureus*, (B) *Pseudomonas aeruginosa*

Optimum conditions for rhamnolipid Production: In order to boost the production of rhamnolipid from selected the producer isolate (PO10), optimization was required before scale up production process. Two essential factors were studied to enhance the production process carbon and nitrogen sources, while the physical parameters that we're not investigated in this study, have been adjusted according to recent previous studies such as optimum temperature (30°C) (21), pH =7 (21), agitation rate 120rpm (Shaban, 2016).

Optimization of carbon source: Different carbon sources were investigated for

Iraqi Journal of Agricultural Sciences –2026:57(8):2113-2132
P-ISSN: 0075- 0530 /E-ISSN: 2410-0862
DOI: https://doi.org/10.36103/vpe69p76

biosurfactant production by *P.aeruginosa* PO10. The results provided in Figure 2 showed that the olive oil was the best carbon source for biosurfactant production with E24% (67 %). The used of olive oil shown to be more effective substrate for rhamnolipids production by *P. aeruginosa* than glycerol, glucose and both together according to study by Maier (Marangon *et al*., 2020).

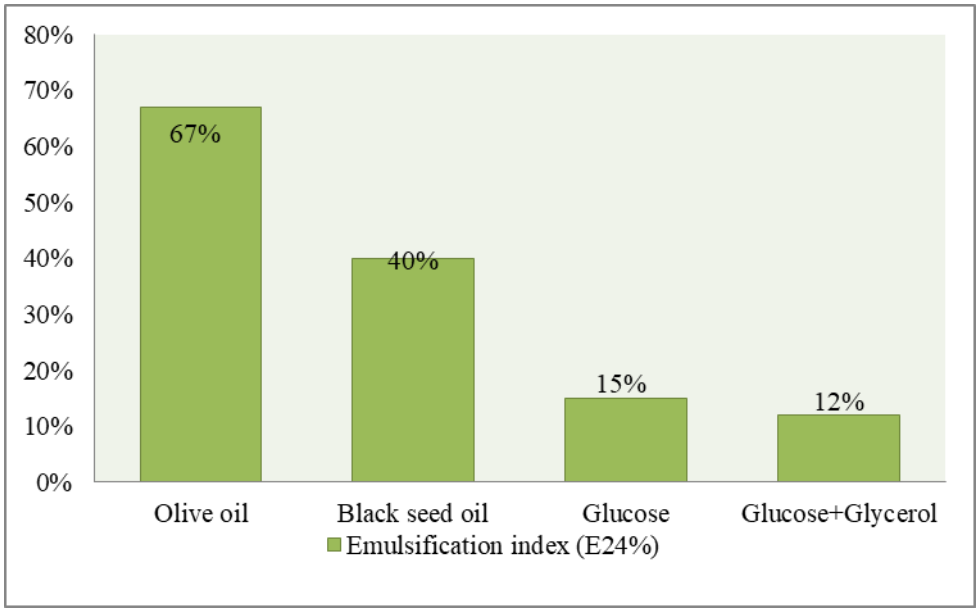

Figure 2. The effect of carbon sources on RL production from PO10 isolate

Optimization of nitrogen source: Different nitrogen sources were utilized to estimate the best nitrogen source for RL production, with best carbon source that previously identified the result showed that yeast extract was the best nitrogen source with emulsification index of 70% as shown in figure 3. Yeast extract serve as an excellent nitrogen source for biosurfactant production, due to its rich composition of proteins, amino acids and essential trace elements (Fontes *et al*., 2010).

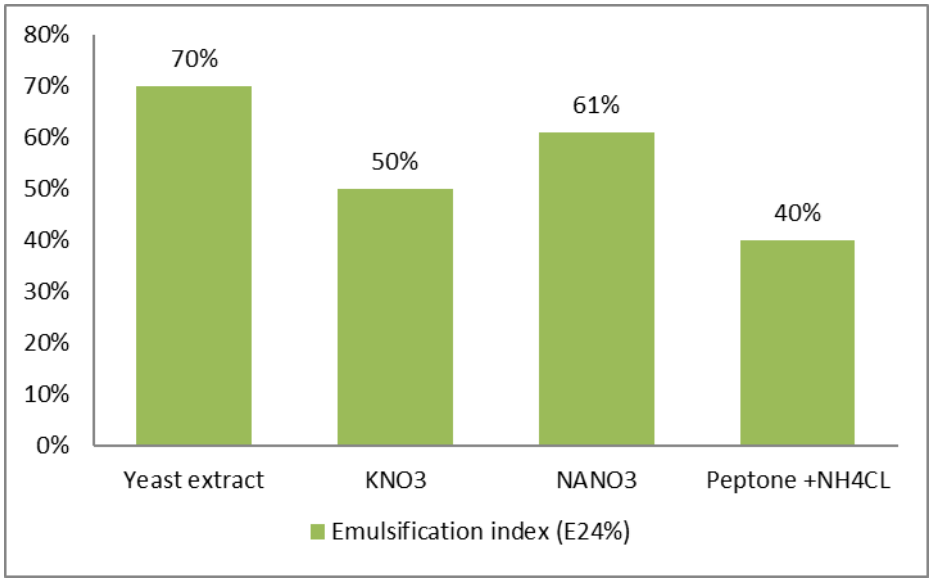

Figure 3. The effect of nitrogen sources on RL production from PO10 isolate

Extraction and purification of rhamnolipid: The results from the optimization experiments were used in order to reach the maximum yield of RL from cell free supernatant by used the (chloroform: methanol) solvent system at ratio (2:1 v/v), due to their ability to dissolve wide range of organic compounds including lipids and proteins (Sana *et al*., 2018). For purification, Silica gel chromatography is considered the common technique used for the purification of crude rhamnolipid. Figure 4 represent the emulsification index and fraction

Iraqi Journal of Agricultural Sciences –2026:57(8):2113-2132
P-ISSN: 0075- 0530 /E-ISSN: 2410-0862
DOI: https://doi.org/10.36103/vpe69p76

number as a result for the mentioned process. With flow rate 3ml/9min, peaks of rhamnolipid appeared between fraction number (8-15) stating with 76% to 45% of emulsification activity. Fractions that give a positive result for presence of rhamnolipid according to E24% were collected and dried to obtain purified rhamnolipid and use in remaining experiments.

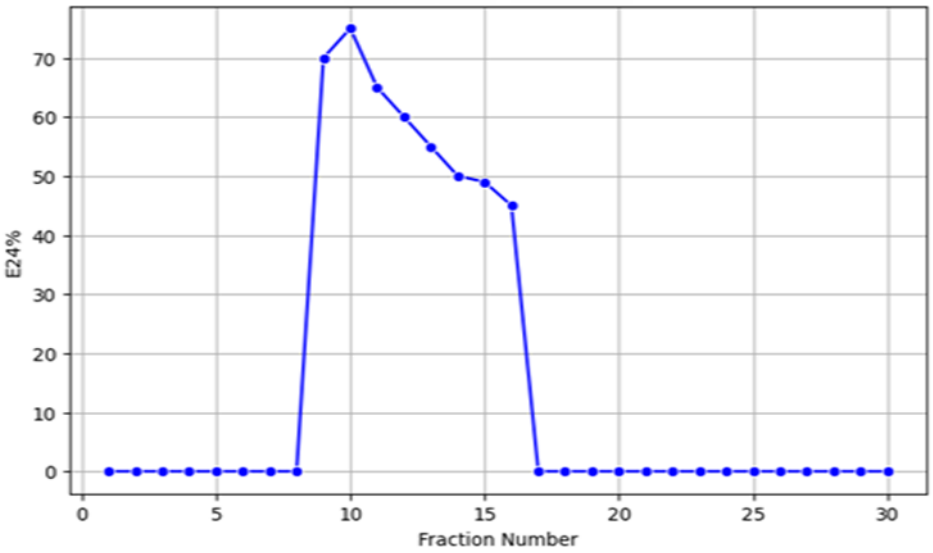

Figure 4. Purification of rhamnolipid produced by *P.aeruginosa,* E24% variation across fractions.

Characterization of Rhamnolipid FTIR Analysis: FTIR is a traditional technique used to determine the chemical bonds and the functional groups present in a substrate. These functional groups are represented by peaks at specific wavelength, as different groups vibrate by absorbing particular frequencies when irradiated with infrared light (Sudarshan *et al*., 1992). According to (figure 8/A), many major peaks appeared in spectrum of rhamnolipid; the peaks in the range between (1300-1000) cm^{-1} were typically attributed to the C-O stretching bands formed between carbon and hydroxyl groups of rhamnose rings. The stretching bands of carboxylic acids were typically represented by peaks around 1740-1500 cm^{-1}. At 1560 cm^{-1}, the band corresponds to the COO of the rhamnolipid. Peak at 1461 cm^{-1} related to the (CH) group of rhamnolipid. Also, the C-H stretching bands of CH, CH2 and CH3 groups were observed at 2854, 2925 and 3000 cm^{-1}. The absorption peak at 1051 cm^{-1} was attributed to the C-O-C bond in the rhamnose molecule within glycolipid. Finally, the band in the range of (3200-3500) cm^{-1} indicated the presence of free –OH groups, resulting from hydrogen bonding in poly saccharides and OH stretching of carboxylic acid groups. Absorption bands around 1712 cm^{-1} and 1645 cm-1 represent ester and carbonyl groups (C=O). All of the mentioned functional groups observed in this test confirm the presence of rhamnolipid biosurfactant.

GC-MS Analysis: GC-MS chromatogram of rhamnolipid showed major peaks indicating the presence of essential rhamnolipid compounds (figure 5). The major peaks of compounds at different retention time 23.585, 25.046, 25.157, 26.057, and 26.201 minutes were identified from standard library compound as n-Hexadecanoic acid, 9,12 Octadecadienoic acid, cis-13-Octadecenoic acid,methyl ester, 9-Octadecenoic acid, (E)-, Octadecanoic acid. As a result, the GC-MS analysis indicates the presence and structure of the major rhamnolipid components.

Iraqi Journal of Agricultural Sciences –2026:57(8):2113-2132
P-ISSN: 0075- 0530 /E-ISSN: 2410-0862
DOI: https://doi.org/10.36103/vpe69p76

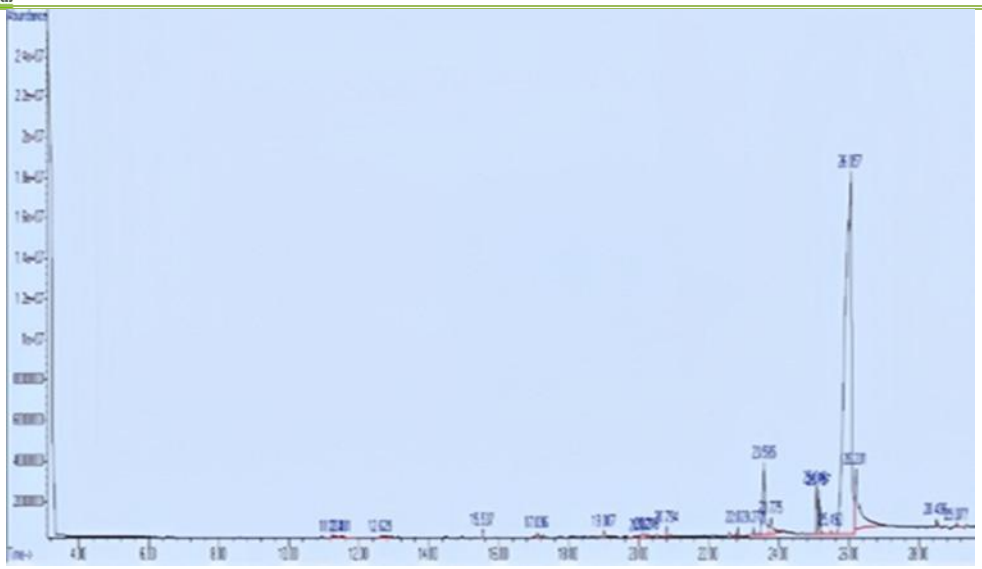

Figure 5. GC-MS analysis of rhamnolipid produced by *P.aeruginosa* PO10

Determination of minimum inhibitory concentration for rhamnolipid (MIC): It was obtained that 12.5 mg/ml was the MIC for both tested isolates *P.aeruginosa* and *S.aureus*. The findings highlight that rhamnolipid is a promising antibacterial agent against both Gram-positive and Gram-negative bacteria. Rhamnolipid are likely to aggregate within bacterial membranes, leading to the formation of transmembrane pores. These pores function as channels, enhancing the permeability of the cell to the periplasm (Lovaglio *et al*., 2011).

Antibacterial activity of rhamnolipid: Antibacterial activity of rhamnolipid was tested against two clinical isolates, *P.aeruginosa* and *S.aureus*, which were isolated from burns and wounds infection and appeared multidrug resistance to antibiotics. The results, shown in Table 2, indicate varying antibacterial capability of rhamnolipid against pathogenic bacteria, with concentration ranged from 25 to 100 mg/ml. The inhibition zone diameter obtained against *P. aeruginosa* ranged from 18 to 20.7 mm, while for *S. aureus*, it ranged from 19.5 to 21.5 mm.

Table 2. Antibacterial activity of rhamnolipid produced by *pseudomonas aeruginosa* PO10 against pathogenic bacteria

Rhamnolipid mg/ml	*P. aeruginosa*(mm)	*S. aureus* (mm)
25	18	19.5
50	18.1	21
75	20.6	21.3
100	20.7	21.5

The primary antibacterial mechanism of rhamnolipid involves bacterial membrane disruption. Due to their surface-active properties, rhamnolipid molecules can interact with the lipid bilayer of bacterial cell membranes, compromising their integrity. This interaction can cause loss of the cellular homeostasis, leakage of intracellular components and ultimately cell death (Sánchez *et al*., 2007). The present findings are in agreement with those reported (King *et al*., 1991), who found that concentration ranging from 25 to 200mg/ml of the partially purified lipopeptides biosurfactant from *L. plantarum* Z9 resulted in inhibition zones of 14-28 mm against *P. aeruginosa* and 13-29 mm against *S. aureus*. This similarity suggests that rhamnolipids exhibit a comparable antibacterial effect within similar concentration ranges.

Biofriendly Chitosan Nanoparticles Encapsulated Rhamnolipid (C/RL-NPs): C/RL-NPs were synthesized using the ionic gelation method, primarily relies on tripolyphosphate (TPP) as a cross-linking agent. Several mechanisms explain the formation of smaller and more stable nanoparticles in presence of rhamnolipid. Chitosan contains a greater number of NH3+ groups compared to rhamnolipid, which may

Iraqi Journal of Agricultural Sciences –2026:57(8):2113-2132
P-ISSN: 0075- 0530 /E-ISSN: 2410-0862
DOI: https://doi.org/10.36103/vpe69p76

contribute to the presence of freer NH3+ groups. In addition to electrostatic interactions, rhamnolipid can also facilitate secondary interactions, such as hydrogen bonding between the hydroxyl (OH) groups of both chitosan and rhamnolipid. The addition of rhamnolipid enhances the stabilization of chitosan within nanoparticles, leading to higher loading efficiency, smaller and more uniform particle size, and improved stability compared to C-NPs (Mnif *et al*., 2018).

Characterization of C/RL-NPs UV-Visible spectroscopy: The primary step in confirmation of the synthesis of C/RL-NPs is the UV-visible spectroscopy test. The absorbance of rhamnolipid, chitosan and C/RLNPs were measured. The chitosan exhibited a peak at 300 nm with an absorbance of 0.422, and another peak at 226 nm with an absorbance of 3.05. The rhamnolipid showed a peak at 265 nm with an absorbance of 0.588. For C/RL-NPs, peaks were observed at 350nm (0.191 absorbance), 263 nm (1.184 absorbance), and 258 nm (2.324 absorbance). In the chitosan the highest absorbance value was 3.05, while the lowest absorbance value was 0.422 at wavelength 226nm and 300 nm, respectively. Furthermore, the absorbance value of rhamnolipid was 0.588 at wavelength 265nm. In case of C/RL-NPs the highest absorbance value was 2.324 and the lowest absorbance value was 0.191 at wavelength 258 nm and 350 nm, respectively. These results show the differences in the absorbance, which indicate for the formation of the of C/RL nanoparticles. The obtained results of UV analysis showed in figure 6.

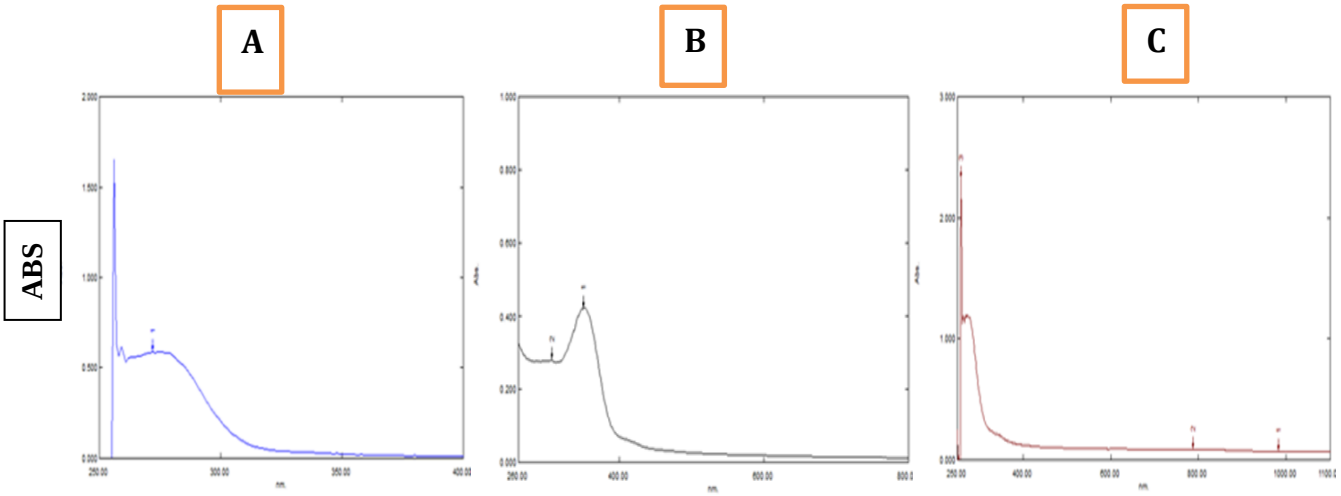

Figure 6. UV-Vis Analysis of (A) Rhamnolipid (B) Chitosan, (C) C/RL-NPs

Zeta potential measurement: Zeta potential is an essential parameter for classifying of stability of nanoparticles. As shown in figure 7, the C/RL-NPs exhibit a positive zeta potential value. The sharp peak at +39 mV confirming the encapsulation of rhamnolipid, and this result is in agreement with (Mnif *et al*., 2018) and shows a more positive zeta potential value compared to (Bettencourt *et al*., 2021). indicating more stable particles. For more stable nanoparticles, the zeta potential of the nanoparticles should be either highest than +30mV or lower than -30 mV (Shah *et al*., 2015).

Iraqi Journal of Agricultural Sciences –2026:57(8):2113-2132
P-ISSN: 0075- 0530 /E-ISSN: 2410-0862
DOI: https://doi.org/10.36103/vpe69p76

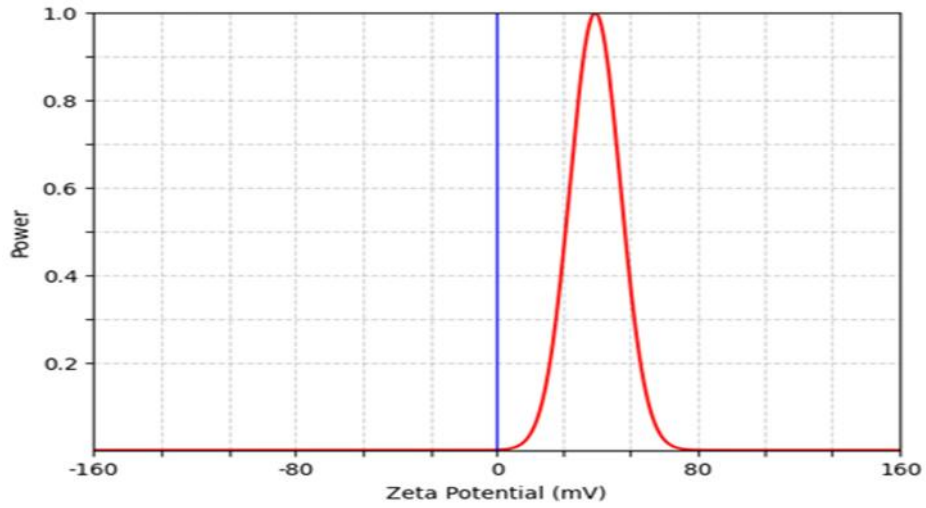

Figure 7. Zeta potential measurement of C/RL-NPs

Fourier transformation infrared spectroscopy (FTIR): FTIR analysis was utilized to identify the functional groups responsible for reducing chitosan to CSNPs encapsulated rhamnolipid and ensuring their stabilization. The FTIR analysis of the samples was conducted within the range of 400-4000 cm-1. Figure 8 present the results. The shift of the O-H and N-H stretching band (3461/3226 cm^{1}) to 3309 cm^{1} indicates hydrogen bonding. The presence of rhamnolipid in the nanoparticles was confirmed by retained C-H stretching bands (2937/2779 cm^{1}) and the C=C stretching peak at 1645 cm^{1}. Electrostatic interactions between chitosan's amide and rhamnolipids carboxyl groups were suggested by the shift of the amide I band from 1650 cm^{1} to 1645 cm^{1}. The N-H bending peak shifted from 1564 cm^{1} to 1577 cm^{1}, confirming nanoparticle formation. The C=O stretching of the ester group (1739 cm^{1}) showed disappearance/broadening, indicating interaction or partial coverage of rhamnolipid. Additionally, shifts in the C-N (1413 to 1330 cm^{1}) and C-O stretching bands (1076 to 1085 cm^{1}) suggest structural modifications in the chitosan network due to nanoparticle formation.

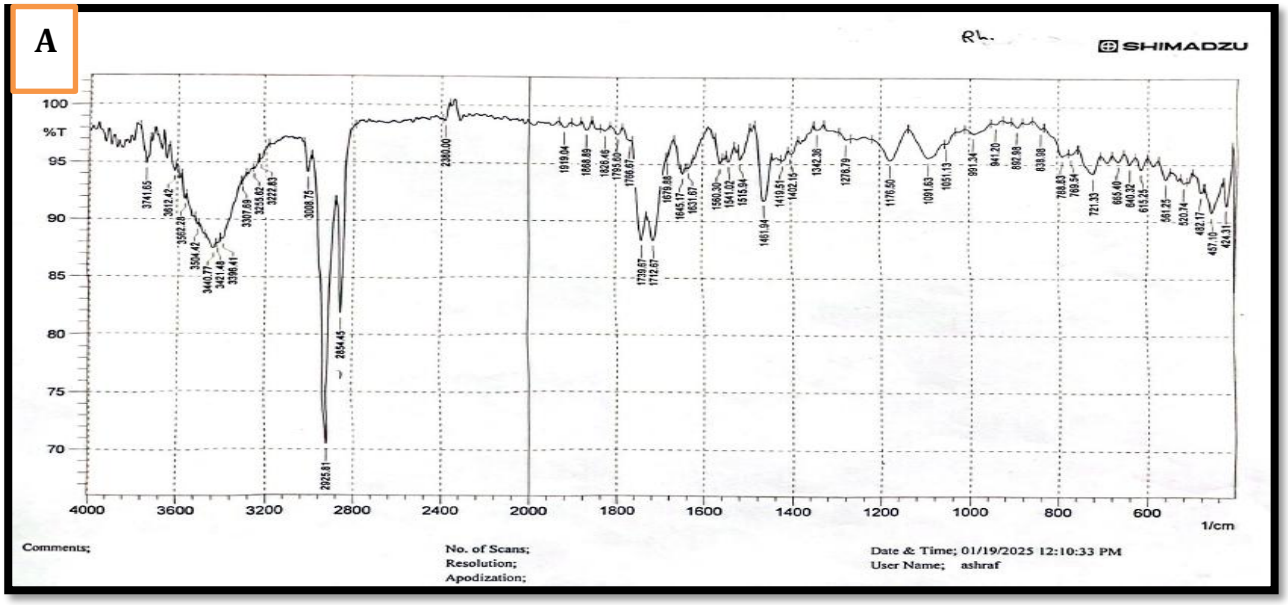

Iraqi Journal of Agricultural Sciences –2026:57(8):2113-2132
P-ISSN: 0075- 0530 /E-ISSN: 2410-0862
DOI: https://doi.org/10.36103/vpe69p76

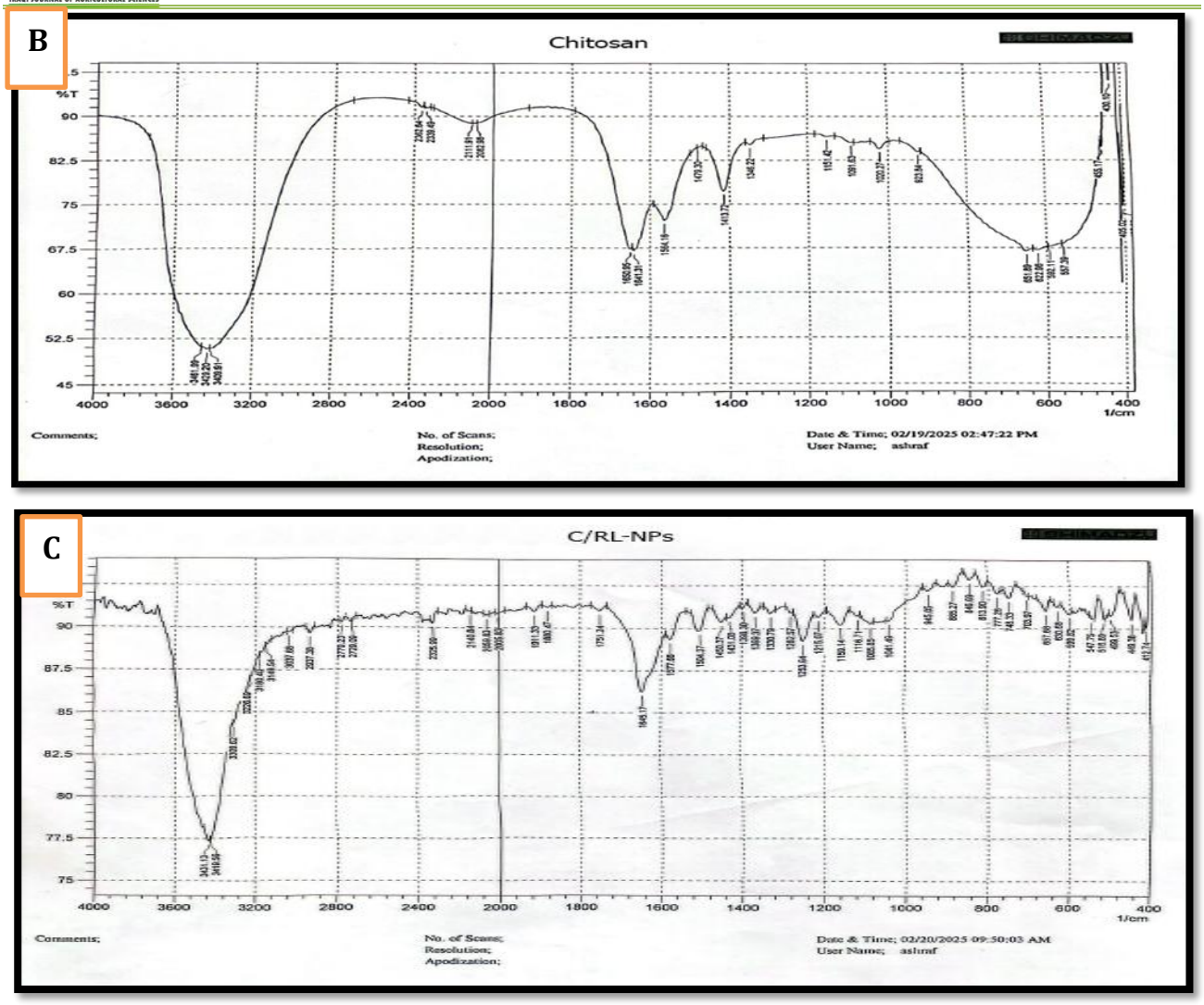

Figure 8. FTIR measurements of (A) Rhamnolipid, (B) Chitosan, (C) C/RL-NPS

Field Emission Scanning Electron Microscopy (FESEM): The morphology of C/RL-NPs was analyzed using filed emission scanning electron microscope (FESEM), the results are shown in figure 9. C/RL-NPs exhibited a spherical shape with diameter range of 44.78-60.71 nm, and displayed a relatively homogeneous morphology.

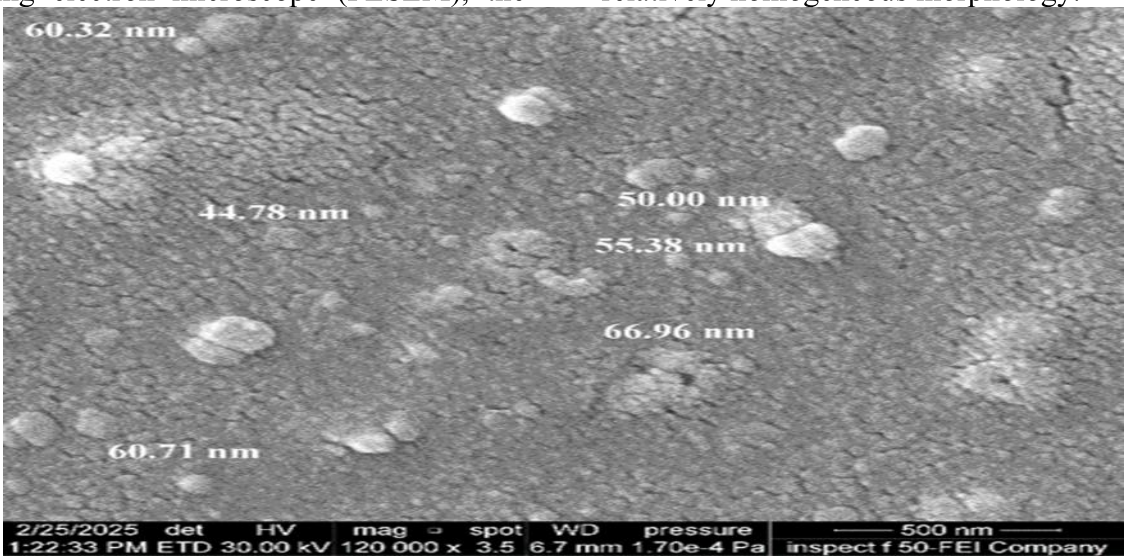

Figure 9. Filed Emission Scanning Electron Microscopy image of C/RL-NPs.

Iraqi Journal of Agricultural Sciences –2026:57(8):2113-2132
P-ISSN: 0075- 0530 /E-ISSN: 2410-0862
DOI: https://doi.org/10.36103/vpe69p76

Atomic Force Microscope (AFM)

Atomic force microscope (AFM) is use to study the changes in morphology and particle size (Sundar *et al*., 2010). The size of C/RL-NPs was estimated by using AFM shown in figure 10. The result shows that the average size of C/RL-NPs was 71.6 nm. The synthesized C/RL-NPs in this study exhibit a smaller size of 71 nm, compared to the larger size of 329 nm reported in (Bettencourt *et al*., 2021). The smaller size can be considered an advantage, as it may lead to enhanced surface area and improved properties for various applications, such as better interaction with biological systems or more efficient delivery of active compounds.

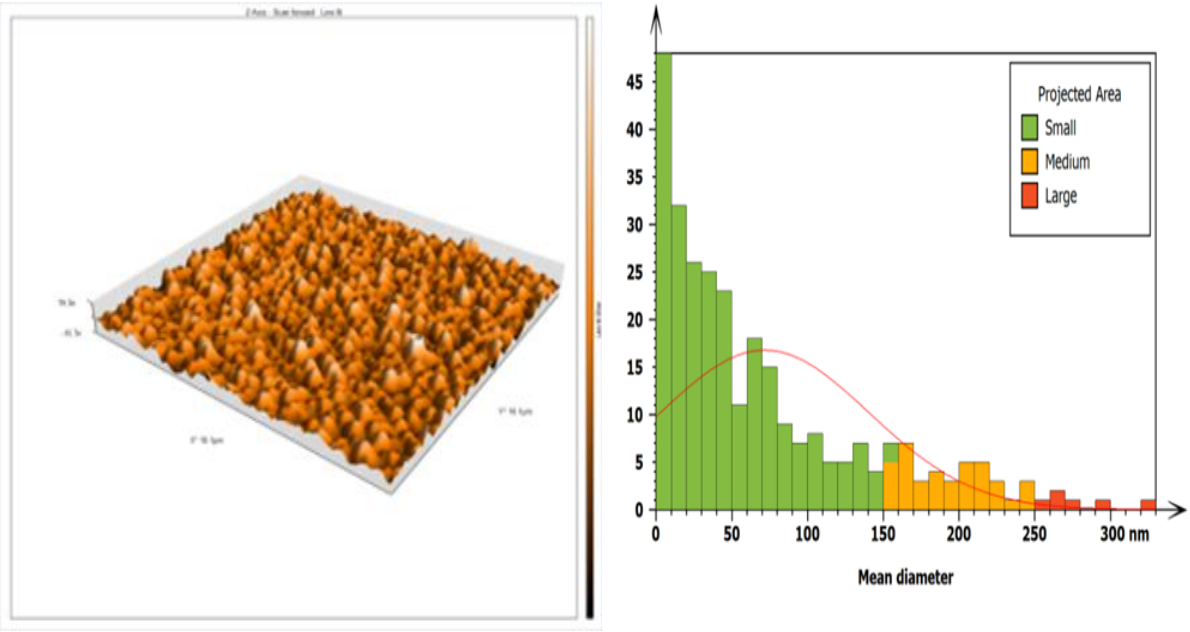

Figure 10. 3D AMF image of synthesis C/RL-NPs with NPs size analysis curve

C/RL-NPs as Antibacterial Agent: Determination of minimum inhibitory concentration for C/RL-NPs (MIC): In order to determine the antibacterial activity of C/RL-NPs, this formula was examined against both Gram negative (*P.aeruginosa*) and Gram positive (*S.aureus*) bacteria, using microtiter plate method. The results showed that, the produced component can inhibit bacterial growth in vitro, compared to the growth of non-treated bacteria (positive control). The negative control which contained only the medium without bacteria, confirmed that no contamination occurred. It was obtained that the MIC for Gram-negative *P.aeruginosa* and Gram-positive *S.aureus* was 1.25mg/ml. The MIC value of free rhamnolipid was 12.5mg/ml, whereas the MIC of C/RL-NPs was significantly reduced to 1.25 mg/ml. This 10-fold reduction highlights the enhanced antibacterial activity of C/RL-NPs, likely due the synergistic effect of chitosan and rhamnolipid as nanoparticles. The nanofromulation improved bacterial membrane interaction, increased stability and enhanced bioavailability, leading to greater efficacy at lower concentration (Irfan *et al*., 2015). much more chitosan free amino groups in the C/RL-NPs cause higher charge density and thereby a potential boost of chitosan antibacterial activity, which relies on electrostatic interaction with anionic components of the bacterial wall and membrane (Thanomsub *et al*., 2006).

Antibacterial activity of C/RL-NPs

The antibacterial activity of C/RL-NPs was examined using the well diffusion method. Different concentrations of the nanocomposite were used to evaluate the inhibition zone obtained and its ability to combat both Gram-positive *S.aureus* and Gram-negative *P.aeruginosa* (Table 3). The mechanism of action of chitosan is based on electrostatic interactions between the polymer and the polyanionic acids and teichoic acids found in the thick peptidoglycan layer of the cell walls of gram-positive bacteria, which can result in cell wall disruption (Sana *et al*., 2018). An

Iraqi Journal of Agricultural Sciences –2026:57(8):2113-2132
P-ISSN: 0075- 0530 /E-ISSN: 2410-0862
DOI: https://doi.org/10.36103/vpe69p76

interesting observation was that when rhamnolipid and chitosan is combined onto nanoparticles, an antibacterial synergistic effect was achieved. This was evident as the amount of rhamnolipid in the tested C/RL-NPs was 10 times lower (1.25 mg/ml) than in free rhamnolipid (12.5 mg/ml). This enhanced antibacterial activity may be attributed to the positive charge of chitosan in C/RL-NPs, which attracts the negatively charged *S.aureus* (Qazi *et al*., 2013). Also, encapsulated drugs can exhibit much more stability favouring their inclusion onto the bacterial cell (Maier & Soberón-Chávez, 2000). The antibacterial activity of C/RL-NP-s is primarily driven by rhamnolipid, which targets the bacterial cell membrane, leading to increased permeability and subsequent cell damage (Bharali *et al*., 2013).

Table 3. Comparative Antibacterial Activity of C/RL-NPs against *P.aeruginosa* and *S.aureus*

Tested Conc.	***P.aeruginosa* (mm)**	***S. aureus* (mm)**
	C/RL-NPs	**C/RL-NPs**
2500µg/ml	20	22.6
1250µg/ml	16.8	17.5
625µg/ml	15.6	15.7
312µg/ml	14	14.5
156µg/ml	10	12

The Synergistic Effect of C/RL-NPs in Combination with Selected Antibiotics: To the best of our knowledge, this is the first study to investigate and discuss the synergistic effect of C/RL-NPs in combination with selected antibiotics. This novel approach explores the potential enhancement of antibacterial activity through the interaction between C/RL-NPs and conventional antibiotics, providing new insights into their combined efficacy against pathogenic bacteria. Agar plate method was used to investigate the synergistic effect of C/RL-NPs and selected antibiotics against both Gram-positive *S.aureus* and Gram-negative *P.aeruginosa*. In case of *P.aeruginosa*, its exhibited moderate resistance against ciprofloxacin, with an inhibition zone of 23 mm. However, when combined with C/RL-NPS, the inhibition zone increased to 34mm. This result suggests a shift from moderate resistance to susceptibility when ciprofloxacin was used in combination with C/RL-NPs. Similarly, the combination of C/RL-NPs with Gentamicin resulted in a significant increase in the inhibition zone, shifting from no inhibition zone with persist cells (Gentamicin only) to 35mm. likewise, for Ceftazidime showed high degree of with no inhibition zone, while showed 19 mm for tested Ceftazidime with nanocomposite. In comparable manner, the combination of C/RL-NPs with Azteronam led to a notable antibacterial effect, as Azteronam alone showed no inhibition zone, whereas the combination resulted in 18.5mm zone. Additionally, Piperacillin-Tazobactam, which initially exhibited an inhibition zone of 11.6mm, demonstrated a remarkable increase to 37mm upon combination with C/RL-NPs. These findings reinforce the potential of C/RL-NPs to enhance the antibacterial efficacy of certain antibiotics against multi-drug resistance *P.aeruginosa*. For Gram-positive *S.aureus*, a significant enhancement in antibacterial activity was observed when C/RL-NPs were combined with selected antibiotics. Doxycycline alone exhibited an inhibition zone of 10 mm, which increased remarkably to 35 mm in combination with C/RL-NPs. Similarly, Azithromycin showed no inhibition alone, yet when combined with C/RL-NPs, the inhibition zone expanded to 33 mm. A comparable trend was observed with Nitrofurantoin and Linezolid, where no inhibition zones were detected when used alone, but upon combination with C/RL-NPs, they exhibited zones of 15 mm and 16 mm, respectively. An interesting observation was noted with Trimethoprim, the combination did not result in a notable enhancement compared to C/RL-NPs alone, which showed an inhibition zone of 15 mm. this suggests a different interaction mechanism. Unlike other antibiotics that act on the bacterial ribosomes or bacterial membrane, Trimethoprim targets dihydrofolate reductase (DFHR), an intracellular enzyme essential for folic acid synthesis. Since C/RL-NPs primarily disrupt

Iraqi Journal of Agricultural Sciences –2026:57(8):2113-2132
P-ISSN: 0075- 0530 /E-ISSN: 2410-0862
DOI: https://doi.org/10.36103/vpe69p76

the bacterial membrane, the lack of synergistic effect may be due to Trimethoprim's inability to fully utilize this mechanism or the presence of bacterial resistance factors. Rhamnolipid is a type of glycolipid biosurfactant known for its excellent biodegradability, biocompatibility and low toxicity, as indicate by an acute oral LD50 of over 5000 mg/kg according to United States Environmental protection Agency (PC Code 110029). Many researches have demonstrated its ability not only to disrupt the architecture of biofilms but also to inhibit bacterial adhesion. The primary target of this disruption is the extracellular polymeric substances (EPS), which from dense outermost layer of biofilms and serves as protective barrier against antibiotics. Once the EPS layer degraded, the internal bacteria within the biofilm lose their protection, become dispersed, and gradually regain their susceptibility to antibiotics, making them more vulnerable to antimicrobial treatment (De la Fuente-Núñez *et al*., 2013; Kucukoglu *et al*., 2019).

Table 4. Antibiotics. C/RL-NPs, and combination effect on *P.aeruginosa* and *S.aureus*

Tested ABX	*P.aeruginosa* (mm)		*S. aureus* (mm)	
	ABX	C/RL NPs+ABX	ABX	C/RL-NPs +ABX
AZM	-	-	No zone	33
ATM	No zone	18.5	-	-
CAZ	No zone	19	-	-
CIP	23	34	-	-
DOX	-	-	10	35
GEN	No zone	35	-	-
LZD	-	-	No zone	16
NIT	-	-	No zone	15
TZP	11	37	-	-
TMP	-	-	No zone	No zone

CONCLUSION

Based on the obtained results, the following conclusions were drawn:

1. The local isolate of Pseudomonas aeruginosa isolated from soil contaminated with hydrocarbons is an efficient bacterial isolate in rhamnolipid production with high production in MSM media that contained olive oil as carbon source and yeast extract as nitrogen source with pH 7 for 72 h incubation time at 30°C with agitation rate 120 rpm.
2. Column chromatography with silica gel is a suitable technique for purifying rhamnolipid, also the FTIR and GC-MASS technique is suitable methods for characterization of rhamnolipid.
3. Chitosan nanoparticles encapsulated rhamnolipid can be synthesis using the green method in presence of sodium tri-polyphosphate (TPP) as a cross linker.
4. UV-vis, FESEM, Zeta potential, FTIR, and AFM are accurate techniques that can be used to characterize the produced chitosan nanoparticles encapsulated rhamnolipid.
5. The present study provides significant evidence on the antibacterial activity of rhamnolipid and chitosan encapsulated rhamnolipid in nanoparticles against MDR Pseudomonas aeruginosa and Staphylococcus aureus which considered as the main cause of burns and wounds infections.
6. One of the most important findings in this study is the combination of C/RL-NPs with antibiotics enhanced their antibacterial efficacy, against resistance and intermediate – resistance isolates.
7. The combination of C/RL-NPs and antibiotics opens a new approach for treating infections caused by both Gram-negative and Gram- positive bacteria due to their high antibacterial activity.

ACKNOWLEDGEMENT

Firstly, and always, all praise and thanks are due to Allah, the Most Gracious, and the Most Merciful, who granted me the strength, patience, and guidance to complete this work. Without His blessings, none of this would have been possible. I am sincerely grateful to the Dean of the College of Science, University of Baghdad, for giving me the opportunity to pursue my M.Sc. study, and I extend my heartfelt thanks to the administration and staff of the Department of Biotechnology for their continuous assistance and encouragement

Iraqi Journal of Agricultural Sciences –2026:57(8):2113-2132
P-ISSN: 0075- 0530 /E-ISSN: 2410-0862
DOI: https://doi.org/10.36103/vpe69p76

throughout my academic journey. With deep respect and appreciation, I thank my supervisor, Dr. Nadhim Hassan Hayder, Head of the Department of Biotechnology, for his generous guidance, valuable advice, and consistent support. His tireless efforts and mentorship were a source of inspiration and played a vital role in the success of my study. I would also like to extend my sincere thanks to Dr. Sahar Rhyme, Dr. Hiba Abdul-Rahman, for their academic support and kind guidance. To my beloved family, I owe a debt of gratitude that words cannot fully express. Their love, prayers, and unwavering belief in me have been my greatest source of strength. Lastly, I thank every person who extended a hand, offered a kind word, or supported me in any way during this journey. May Allah reward you all with the best.

CONFLICT OF INTEREST

The authors declare that they have no conflicts of interest.

AUTHOR/S DECLARATION

We confirm that all Figures and Tables in the manuscript are original to us. Additionally, any Figures and images that do not belong to us have been incorporated with the required permissions for re-publication, which are included with the manuscript. Author/s signature on Ethical Approval Statement.

Ethical Clearance and Animal welfare

Funds:

REFERENCES

Abouseoud, M., Yataghene, A., Amrane, A., & Maachi, R. (2008). Biosurfactant production by free and alginate entrapped cells of Pseudomonas fluorescens. Journal of Industrial Microbiology & Biotechnology, 35(11), 1303–1308. https://doi.org/10.1007/s10295-008-0411-0

Ahmad, A., Ahmad, I., Ramzan, S., Kiyani, M., Dubal, D., & Mubarak, N. M. (2021). Nanomaterial synthesis protocols. In F. Verpoort, I. Ahmad, A. Ahmad, A. Khan, & C. Y. Chee (Eds.), Nanomedicine Manufacturing and Applications (pp. 37–85). Elsevier. https://doi.org/10.1016/B978-0-12-820773-4.00010-X

Ali, A., & Ahmed, S. (2018). A review on chitosan and its nanocomposites in drug delivery. International Journal of Biological Macromolecules,109,273–286. https://doi.org/10.1016/j.ijbiomac.2017.12.078

.Balouiri, M., Sadiki, M., & Ibnsouda, S. K.(2016). Methods for in vitro evaluating antimicrobial activity: A review. Journal of pharmaceutical analysis, 6(2), 71–79. https://doi.org/10.1016/j.jpha.2015.11.005

Bettencourt, A. F., Tome, C., Oliveira, T., Martin, V., Santos, C., Goncalves, L., ... & Ribeiro, I. A. (2021). Exploring the potential of chitosan-based particles as delivery carriers for promising antimicrobial glycolipid biosurfactants. *Carbohydrate polymers*, *254*, 117433. https://doi.org/10.1016/j.carbpol.2020.117433

Bharali, P., Saikia, J., Ray, A., & Konwar, B. (2013). Rhamnolipid (RL) from *Pseudomonas aeruginosa* OBP1: A novel chemotaxis and antibacterial agent. Colloids and Surfaces B: Biointerfaces, 103, 502–509. https://doi.org/10.1016/j.colsurfb.2012.10.064

Bustelo, M., Pinazo, A., Manresa, M., Mitjans, M., Vinardell, M., & Pérez, L. (2017). Monocatenary histidine-based surfactants: Role of the alkyl chain length in antimicrobial activity and their selectivity over red blood cells. Colloids and Surfaces A: Physicochemical and Engineering Aspects, 532,501–509. https://doi.org/10.1016/j.colsurfa.2017.04.017

Corbett, J. C., McNeil-Watson, F., Jack, R. O., & Howarth, M. (2012). Measuring surface zeta potential using phase analysis light scattering in a simple dip cell arrangement. Colloids and Surfaces A: Physicochemical and Engineering Aspects, 396, 169–176. https://doi.org/10.1016/j.colsurfa.2011.12.065

Costa, E. M., Silva, S., Veiga, M., Baptista, P., Tavaria, F. K., & Pintado, M. E. (2021). Textile dyes loaded chitosan nanoparticles: Characterization, biocompatibility and staining capacity. Carbohydrate Polymers, 251, Article117120. https://doi.org/10.1016/j.carbpol.2020.117120

De la Fuente- 10. De la Fuente-Núñez, C., Reffuveille, F. L., Fernández, L., & Hancock, R. E. W. (2013). Bacterial biofilm development as a multicellular adaptation: Antibiotic resistance and new therapeutic

Iraqi Journal of Agricultural Sciences –2026:57(8):2113-2132
P-ISSN: 0075- 0530 /E-ISSN: 2410-0862
DOI: https://doi.org/10.36103/vpe69p76

strategies. Current Opinion in Microbiology, 16(5), 580–589. https://doi.org/10.1016/j.mib.2013.06.013

Fontes, G. C., Amaral, P. F. F., Nele, M., & Coelho, M. A. Z. (2010). *Factorial design to optimize biosurfactant production by Yarrowia lipolytica*. BioMed Research International, 2010, Article 821306. https://doi.org/10.1155/2010/821306

Grobelny, J., DelRio, F. W., Pradeep, N., Kim, D. I., Hackley, V. A., & Cook, R. F. (2011). Size measurement of nanoparticles using atomic force microscopy. In Characterization of nanoparticles intended for drug delivery (pp. 71-82). Totowa, NJ: Humana Press. https://doi.org/10.1007/978-1-60327-198-1_7

Hussain, S., Joo, J., Kang, J., Kim, B., Braun, G. B., She, Z. G., ... & Ruoslahti, E. (2018). Antibiotic-loaded nanoparticles targeted to the site of infection enhance antibacterial efficacy. *Nature biomedical engineering*, *2*(2), 95-103. https://doi.org/10.1038/s41551-017-0187-5

Irfan, M., Shahi, S. K., & Sharma, P. K. (2015). *In vitro* synergistic effect of biosurfactant produced by *Bacillus subtilis* MTCC 441 against drug-resistant *Staphylococcus aureus*. Journal of Applied Pharmaceutical Science, *5*(3), 113–116. https://doi.org/10.7324/JAPS.2015.50320

Karamchandani, B. M., Maurya, P. A., Dalvi, S. G., Waghmode, S., Sharma, D., Rahman, P. K., ... & Satpute, S. K. (2022). Synergistic activity of rhamnolipid biosurfactant and nanoparticles synthesized using fungal origin chitosan against phytopathogens. Frontiers in bioengineering and biotechnology, 10, 917105. https://doi.org/10.3389/fbioe.2022.917105

King, A. T., Davey, M. R., Mellor, I. R., Mulligan, B. J., & Lowe, K. C. (1991). Surfactant effects on yeast cells. Enzyme and Microbial Technology, 13(2), 148–153. https://doi.org/10.1016/0141-0229(91)90171-6

Kucukoglu, V., Uzuner, H., Kenar, H., & Karadenizli, A. (2019). In vitro antibacterial activity of ciprofloxacin-loaded chitosan microparticles and their effects on human lung epithelial cells. International Journal of Pharmaceutics, 569, Article 118578. https://doi.org/10.1016/j.ijpharm.2019.118578

Lovaglio, R. B., dos Santos, F. J., Junior, M. J., & Contiero, J. (2011). Rhamnolipid emulsifying activity and emulsion stability: pH rules. Colloids and Surfaces B: Biointerfaces, 85(2),301–305. https://doi.org/10.1016/j.colsurfb.2011.03.001

Liu, Y. Y., Wang, Y., Walsh, T. R., Yi, L. X., Zhang, R., Spencer, J., ... & Shen, J. (2016). Emergence of plasmid-mediated colistin resistance mechanism MCR-1 in animals and human beings in China: a microbiological and molecular biological study. The Lancet infectious diseases, 16(2), 161-168. https://doi.org/10.1016/S1473-3099(15)00424-7

Maier, R. M., & Soberón-Chávez, G. (2000). Pseudomonas aeruginosa rhamnolipids: Biosynthesis and potential applications. Applied Microbiology and Biotechnology, 54(5),625–633. https://doi.org/10.1007/s002530000443

Manna, M. S., Tamer, Y. T., Gaszek, I., Poulides, N., Ahmed, A., Wang, X., ... & Toprak, E. (2021). A trimethoprim derivative impedes antibiotic resistance evolution. Nature communications, 12(1), 2949. https://doi.org/10.1038/s41467-021-23191-z

Marangon, C. A., Martins, V. C., Ling, M. H., Melo, C. C., Plepis, A. M. G., Meyer, R. L., & Nitschke, M. (2020). Combination of rhamnolipid and chitosan in nanoparticles boosts their antimicrobial efficacy. ACS applied materials & interfaces, 12(5), 5488-5499. https://doi.org/10.1021/acsami.9b19253

Mnif, I., Ellouz-Chaabouni, S., & Ghribi, D. (2018). Glycolipid biosurfactants: Main classes, functional properties, and related potential applications in environmental biotechnology. Journal of Polymers and the Environment, 26(6), 2192–2206. https://doi.org/10.1007/s10924-017-1076-4

Pasieczna-Patkowska, S., Cichy, M., & Flieger, J. (2025). Application of Fourier Transform Infrared (FTIR) Spectroscopy in Characterization of Green Synthesized Nanoparticles. Molecules, 30(3), 684. https://doi.org/10.3390/molecules30030684

Niladevi, K. N., & Prema, P. (2005). Mangrove actinomycetes as the source of

Iraqi Journal of Agricultural Sciences –2026:57(8):2113-2132
P-ISSN: 0075- 0530 /E-ISSN: 2410-0862
DOI: https://doi.org/10.36103/vpe69p76

ligninolytic enzymes. Actinomycetologica, 19(2),40–47.
https://doi.org/10.3209/saj.19.40

Ohikhena, F. U., Wintola, O. A., & Afolayan, A. J. (2017). Evaluation of the antibacterial and antifungal properties of Phragmanthera capitata (Sprengel) Balle (Loranthaceae), a mistletoe growing on rubber tree, using the dilution techniques. The Scientific World Journal, 2017, Article 9658598.
https://doi.org/10.1155/2017/9658598

Pan, C., Qian, J., Zhao, C., Yang, H., Zhao, X., & Guo, H. (2020). Study on the relationship between crosslinking degree and properties of TPP crosslinked chitosan nanoparticles. Carbohydrate Polymers, 241, Article116349.
https://doi.org/10.1016/j.carbpol.2020.116349

Paulino, B. N., Pessôa, M. G., Mano, M. C. R., Molina, G., Neri-Numa, I. A., & Pastore, G. M. (2016). Current status in biotechnological production and applications of glycolipid biosurfactants. Applied Microbiology and Biotechnology, 100, 10265–10293.
https://doi.org/10.1007/s00253-016-7980-z

Pontes, C., Alves, M., Santos, C., Ribeiro, M. H., Gonçalves, L., Bettencourt, A. F., & Ribeiro, I. A. (2016). Can Sophorolipids prevent biofilm formation on silicone catheter tubes?. International Journal of Pharmaceutics, 513(1-2), 697-708.
https://doi.org/10.1016/j.ijpharm.2016.09.074

Prabaharan, M., & Mano, J. F. (2005). Chitosan-based particles as controlled drug delivery systems. Drug Delivery, 12(1), 41–57.
https://doi.org/10.1080/10717540590889781

Qazi, M. A., Malik, Z. A., Qureshi, G. D., Hameed, A., & Ahmed, S. (2013). Yeast extract as the most preferable substrate for optimized biosurfactant production by rhlB gene-positive Pseudomonas putida SOL-10 isolate. Journal of Bioremediation & Biodegradation,4(2).

. Raafat, D., von Bargen, K., Haas, A., & Sahl, H.-G. (2008). Insights into the mode of action of chitosan as an antibacterial compound. Applied and Environmental Microbiology, 74(12), 3764–3773.
https://doi.org/10.1128/AEM.00453-08

Sana, S., Datta, S., Biswas, D., & Sengupta, D. (2018). Assessment of synergistic antibacterial activity of combined biosurfactants revealed by bacterial cell envelope damage. Biochimica et Biophysica Acta (BBA) - Biomembranes, 1860(2), 579–585.
https://doi.org/10.1016/j.bbamem.2017.09.027

Sánchez, M., Aranda, F. J., Espuny, M. J., Marqués, A., Teruel, J. A., Manresa, Á., & Ortiz, A. (2007). Aggregation behaviour of a dirhamnolipid biosurfactant secreted by Pseudomonas aeruginosa in aqueous media. Journal of colloid and interface science, 307(1), 246-253.
https://doi.org/10.1016/j.jcis.2006.11.041

Santa Anna, L. M., Sebastian, G. V., Menezes, E. P., Alves, T. L. M., Santos, A. S., Pereira Jr., N., & Freire, D. M. G. F. (2002). Production of biosurfactants from Pseudomonas aeruginosa PA1 isolated in oil environments. Brazilian Journal of Chemical Engineering,19(2),159–166.
https://doi.org/10.1590/S0104-66322002000200011

Shaban, S. M. (2016). Studying the effect of newly synthesized cationic surfactant on silver nanoparticles formation and their biological activity. Journal of Molecular Liquids, 216,137–145.
https://doi.org/10.1016/j.molliq.2015.12.098

Shah, M., Fawcett, D., Sharma, S., Tripathy, S. K., & Poinern, G. E. J. (2015). Green synthesis of metallic nanoparticles via biological entities. Materials, 8(11), 7278–7308.
https://doi.org/10.3390/ma8115377

Sundar, S., Kundu, J., & Kundu, S. C. (2010). Biopolymeric nanoparticles. Science and Technology of Advanced Materials, 11(1).
https://doi.org/10.1088/1468-6996/11/1/014104

Shekhar, S., Sundaramanickam, A., & Balasubramanian, T. (2015). Biosurfactant producing microbes and their potential applications: A review. Critical Reviews in Environmental Science and Technology, 45(14),1522–1554.
https://doi.org/10.1080/10643389.2014.955631

Sifour, M., Al-Jilawi, M. H., & Aziz, G. M. (2007). Emulsification properties of biosurfactant produced from Pseudomonas aeruginosa RB28. Pakistan Journal of

Iraqi Journal of Agricultural Sciences –2026:57(8):2113-2132
P-ISSN: 0075- 0530 /E-ISSN: 2410-0862
DOI: https://doi.org/10.36103/vpe69p76

Biological Sciences, 10(8), 1331–1335. https://doi.org/10.3923/pjbs.2007.1331.1335

Singh, N., Pemmaraju, S. C., Pruthi, P. A., Cameotra, S. S., & Pruthi, V. (2013). Candida biofilm disrupting ability of di-rhamnolipid (RL-2) produced from Pseudomonas aeruginosa DSVP20. Applied Biochemistry and Biotechnology, 169(8), 2374–2391. https://doi.org/10.1007/s12010-013-0149-7

Sudarshan, N., Hoover, D. G., & Knorr, D. (1992). Antibacterial action of chitosan. Food Biotechnology,6(3),257–272. https://doi.org/10.1080/08905439209549838

Thanomsub, B., Pumeechockchai, W., Limtrakul, A., Arunrattiyakorn, P., Petchleelaha, W., Nitoda, T., & Kanzaki, H. (2006). Chemical structures and biological activities of rhamnolipids produced by Pseudomonas aeruginosa B189 isolated from milk factory waste. Bioresource Technology, 97(18),2457–2461. https://doi.org/10.1016/j.biortech.2005.10.029

Varvaresou, A., & Iakovou, K. (2015). Biosurfactants in cosmetics and biopharmaceuticals. Letters in Applied Microbiology,61(3),214–223. https://doi.org/10.1111/lam.12440

Vatanparast, H., Shahabi, F., Bahramian, A., Javadi, A., & Miller, R. (2018). The role of electrostatic repulsion on increasing surface activity of anionic surfactants in the presence of hydrophilic silica nanoparticles. Scientific Reports, 8(1), 7251. https://doi.org/10.1038/s41598-018-25493-7

Iraqi Journal of Agricultural Sciences –2026:57(8):2113-2132
P-ISSN: 0075- 0530 /E-ISSN: 2410-0862
DOI: https://doi.org/10.36103/vpe69p76

التأثير التآزري للرامنوليبيد المنتج بواسطة بكتيريا الزائفة الزنجارية المقيد بالجسيمات النانوية و الكيتوسان مع بعض المضادات الحيوية ضد الممرضات الجلدية المقاومة لمضادات الحياة.

اسامة اكرم داخل ، ناظم حسن حيدر
قسم التقنيات الاحيائية، كلية العلوم، جامعة بغداد.

المستخلص

هدفت هذه الدراسة الى تنقية وتوصيف الرامنوليبيد المنتج من عزلة بيئية لبكتيريا *P.aeruginosa*, وتقييم نشاطه الضد بكتيري بمفرده وعند دمجه مع الكيتوسان على شكل جسيمات نانوية. أظهرت العزلة نشاط تحلل قوي للدم على وسط اجار الدم (منطقة شفافة بقطر 36.6 ملم), ودليل استحلاب مرتفع (E24%=66). تم استخلاص وتنقية الرامنوليبيد باستخدام نظام مذيبات الكلوروفورم:ميثانول (1:2) وتنقيته بواسطة كروماتوغرافيا عمود السيليكا (3.5 x 30 سم) , وتم توصيفه باستخدام تقنية FTIR و GC-MS التي اكدت وجود العناصر الاساسية للرامنوليبيد. بلغت قيم التركيز المثبط الأدنى (MIC) للرامنوليبيد 12.5ملغم/مل لكل من *P.*aeruginosa و *S.aureus*. تم تحضير الجسيمات النانوية من خليط الكيتوسان والرامنوليبيد بطريقة الترسيب الايوني, وتم توصيفها باستخدام التحليل الطيفي للأشعة فوق البنفسجية –المرئية (UV-vis), وتحليل FTIR, ومجهر القوة الذرية AFM, وجهد زيتا Zeta potential الذي بلغ 39+mV, والمجهر الألكتروني الماسح FESEM التي أظهرت أن الجسيمات كروية الشكل ويتراوح حجمها بين 44.78-60.71 نانومتر, حيث اكدت جميع هذه الفحوصات نجاح تصنيع الجسميات النانوية من الكيتوسان والرمنوليبيد وبأستقرارية عالية. انخفضت قيمة MIC للجسيمات النانوية الى 1.25 ملغم/مل. تعد هذه الدراسة الأولى من نوعها التي تبحث في التأثير التآزري للجسيمات النانوية C/RL-NPs عند دمجها مع المضادات الحيوية, وأظهرت النتائج زيادة ملحوظة في أقطار مناطق التثبيط ضد العزلات المرضية من *P.aeruginosa* و *S.aureus* مقارنة بأستخدام المضادات الحيوية أو الجسيمات النانوية بشكل منفرد.

الكلمات المفتاحية: النشاط المضاد للميكروبات ، الكيتوسان، التركيز الحد الأدنى للتثبيط ، الدقائق النانوية، الرامنوليبيد، التأثير التآزري.